Characterizing the Secondary Hydration Shell on Hydrated Myoglobin, Hemoglobin, and Lysozyme Powders by Its Vitrification Behavior on Cooling and Its Calorimetric Glass→Liquid Transition and Crystallization Behavior on Reheating

Günter Sartor, Andreas Hallbrucker, and Erwin Mayer
Institut für Allgemeine, Anorganische, und Theoretische Chemie, Universität Innsbruck, A-6020 Innsbruck, Austria

ABSTRACT For hydrated metmyoglobin, methemoglobin, and lysozyme powders, the freezable water fraction of between ~0.3–0.4 g water/g protein up to ~0.7–0.8 g water/g protein has been fully vitrified by cooling at rates up to ~1500 K min^{-1} and the influence of cooling rate characterized by x-ray diffractograms. This vitreous but freezable water fraction started to crystallize at ~210 K to cubic ice and at ~240 K to hexagonal ice. Measurements by differential scanning calorimetry have shown that this vitreous but freezable water fraction undergoes, on reheating at a rate of 30 K min^{-1}, a glass→liquid transition with an onset temperature of between ~164 and ~174 K, with a width of between ~9 and ~16° and an increase in heat capacity of between ~20 and ~40 J K^{-1} (mol of freezable water)$^{-1}$ but that the glass transition disappears upon crystallization of the freezable water. These calorimetric features are similar to those of water imbibed in the pores of a synthetic hydrogel but very different from those of glassy bulk water. The difference to glassy bulk water's properties is attributed to hydrophilic interaction and H-bonding of the macromolecules' segments with the freezable water fraction, which thereby becomes dynamically modified. Abrupt increase in minimal or critical cooling rate necessary for complete vitrification is observed at ~0.7–0.8 g water/g protein, which is attributed to an abrupt increase of water's mobility, and it is remarkably close to the threshold value of water's mobility on a hydrated protein reported by Kimmich et al. (1990, *Biophys. J.* 58:1183). The hydration level of ~0.7–0.8 g water/g protein is approximately that necessary for completing the secondary hydration shell.

INTRODUCTION

Water in hydrated proteins often is classified according to its freezing/melting behavior as unfreezable water and as freezable water. The former constitutes a hydration range of up to ~0.3–0.4 h (h is defined as gram of water per gram of protein, mass ratio), and it remains mobile down to very low temperatures and does not crystallize even over long periods of time, independent of the rate of cooling or heating (for reviews see Kuntz and Kauzmann, 1974; Cooke and Kuntz, 1974; Rupley and Careri, 1991; Jeffrey and Saenger, 1994). Hydrated water above this hydration range crystallizes on slow cooling but can be vitrified with increasing rates of cooling. We recently reported a study by differential scanning calorimetry (DSC) on the vitrification and crystallization characteristics of freezable water in hydrated methemoglobin (MetHb), of between ~0.4 and 0.7 h, which can be vitrified but crystallizes on heating (Sartor et al., 1992, 1993). One of the conclusions from this study was that the calorimetric glass→liquid transition and crystallization behavior of this vitreous, but freezable, water fraction is clearly different from that of bulk water made by hyperquenching of micron-sized droplets (Johari et al., 1987; Hallbrucker et al., 1989).

We now extend the previous DSC study of hydrated MetHb powders to hydrated metmyoglobin (MetMb) and lysozyme and to higher cooling rates, and we report in this study for the hydration range of up to ~0.8 h the influence of water content, cooling rate, and physical aging, or annealing, on the vitrification of the freezable water fraction on cooling and on the calorimetric glass→liquid transition and crystallization behavior on reheating (from Sartor, 1991, 1994). The vitreous, but freezable, water fraction in hydrated MetMb, MetHb, and lysozyme powders shows very similar calorimetric behavior for the whole hydration range studied here; it undergoes on heating at a rate of 30 K min^{-1} a glass→liquid transition with an onset temperature, or T_g, of between ~164 and ~174 K, an increase in heat capacity in the glass→liquid transition region, or ΔC_p, of ~20–40 J K^{-1} mol^{-1}, and it starts to crystallize to cubic ice at ~200–210 K. Its behavior is very similar to that reported by Hofer et al. (1990, 1992) for the vitreous, but freezable, water fraction of water imbibed in the pores of a synthetic polymer of <30 Å diameter, namely, in poly(2-hydroxyethyl methacrylate; PHEMA) hydrogel (Bosio et al., 1992), but it is clearly different from that of bulk water with a T_g of 136 ± 1 K and a ΔC_p of 1.6 J K^{-1} mol^{-1} obtained for heating at the same rate (Johari et al., 1987; Hallbrucker et al., 1989). The similarity in calorimetric behavior of the vitreous, but freezable, water fraction on the hydrated proteins to that in the synthetic PHEMA hydrogel is suggestive of similar interaction of the water molecules with the polymer's surface. The differences in calorimetric behavior between the vitreous, but freezable, water fraction

Received for publication 3 February 1995 and in final form 21 July 1995.
Address reprint requests to Dr. Erwin Mayer, Inst. fur Allgemeine, Anorganische und Theoretische Chemie, Leopold-Franzens Univ. Innsbruck, A-6020, Innrain 52a Innsbruck, Austria. Tel.: 43-512-507-5110; Fax: 43-512-507-2934; E-mail: erwin.mayer@uibk.ac.at.

0006-3495/95/12/2679/16 $2.00

to that of bulk water are discussed in a phenomenological way and they are attributed to weak perturbation of water's H-bonded network by the protein's surface, which leads to modification of its dynamics.

The vitrification of water-rich protein powders reported here and the characterization of the vitreous and freezable water fraction opens other studies on the dynamics of hydrated proteins as a function of water content and temperature. These studies were confined so far mainly to the vitreous and unfreezable water fraction of up to ~0.3–0.4 h (Morozov and Gevorkian, 1985; Frauenfelder and Gratton, 1986; Parak, 1986; Doster et al., 1986, 1989, 1990, 1991, 1993; Nienhaus et al., 1989; Goldanskii and Krupyanskii, 1989; Smith et al., 1990; Rupley and Careri, 1991; Srajer et al., 1991; Champion, 1992; Pethig, 1992; Pissis et al., 1992; Sartor et al., 1994; Mayer, 1994b), and increasing internal mobility of a protein with increasing hydration has been attributed to water's "plasticizing effect" (Parak, 1986). The further range of hydration that can now be studied at low temperatures in fully vitrified samples up to ~0.7 h by using the cooling rates of this study extends the hydration range for low temperature studies on the dynamics of proteins. We expect in particular that the low temperature ligand rebinding kinetics of photodissociated carbonyl-myoglobin, which depends on the solvent (see, e.g., Doster et al., 1993), is affected by increasing amounts of vitreous water.

Other calorimetric studies of water-protein systems for similar hydration range have been reported and we mention only a few of these by, e.g., Mrevlishvili (1979), Doster et al. (1986), Goldanskii and Krupyanskii (1989), Barkalov et al. (1993), and Czybulka et al. (1993). In these studies the calorimetric features of the vitreous, but freezable, water fraction have not been characterized in the same manner as in this work.

We note that Green et al. (1994) recently reported, for hydrated cytochrome *c* and myoglobin powders containing some freezable water, endothermic steps at similar temperature range of ~160–170 K and attributed these calorimetric features to the onset of a strong water-sensitized β-relaxation due to the protein's side chain rotations. Our arguments against their interpretation and for ours in terms of glass→liquid transition of the vitreous and freezable water fraction will be given in the Discussion.

MATERIALS AND METHODS

Hemoglobin from human blood (No. H 7379) and myoglobin (No. M 0630) were obtained from Sigma Chemical Co. (St. Louis, MO). Both were characterized in aqueous solution (phosphate buffered at pH 6.8) by their UV-visible spectra to be MetHb (Waterman, 1978) and MetMb (Rothgeb and Gurd, 1978) and were used as received. Lysozyme (No. L 6876, from hen egg-white) was also obtained from Sigma Chemical Co.

The proteins were hydrated by keeping over saturated salt solutions at a constant temperature over several weeks (Poole and Finney, 1986). Water content of the as-received proteins, determined by heating to 378 K, was 0.10 h for MetHb and lysozyme and 0.08 h for MetMb. Final water content of the hydrated proteins was determined by weighing to ±0.01 mg, taking into account the water content of the as-received proteins. The hydrated proteins were quickly crimp-sealed into Al pans and weighed. The accuracy of the given hydration values is estimated to be ±0.02 h.

A differential scanning calorimeter (Model DSC-4, Perkin-Elmer Corp., Philadelphia, PA) with a self-written computer program was used for all studies. After the scans were taken, a baseline was subtracted to eliminate curvature of the traces. The data were imported into Origin, a computer program used to prepare the plots (MicroCal Software, Inc., Northampton, MA). Only crimp-sealed Al pans were used to avoid evaporation losses and to obtain a cooling rate of of up to ~150 K min^{-1} in the DSC instrument. Cooling rates of ~1500 and ~2700 K min^{-1} were obtained by dipping sample and Al pan into liquid N_2 or N_2 slush (obtained by pumping on liquid N_2) and by taking the Leidenfrost effect as the indicator that the samples had approached the temperature of liquid N_2. The weights of the samples were between ~10 and 40 mg. The temperature scales in the figures are not corrected for the thermal lag of the instrument (which is 1.5° for heating at a rate of 30 K min^{-1}), but the temperatures given in the text are corrected. Additional experimental details on DSC are given by Sartor et al. (1992), Hofer et al. (1990), Sartor and Mayer (1994), and Hallbrucker et al. (1989).

The x-ray diffractograms were made with samples of hydrated protein powders that were either pressed on the original low temperature sample holder of ~38 g weight (10 mm thickness), which was then cooled at ~250 or ~440 K min^{-1} by dipping the sample holder and sample either into liquid N_2 or into N_2 slush, and thereafter transferred into the precooled low temperature camera. Higher cooling rates of ~1300 or ~1500 K min^{-1} were obtained in liquid N_2 and N_2 slush by reducing the weight and thickness of the sample holder; a thin copper plate of ~5 g weight (2 mm thickness) was used as the sample holder, which after cooling was attached with screws under liquid N_2 onto the appropriately shaped sample holder. These cooling rates were reproducible, and they were determined by attaching firmly a calibrated thermocouple to the holder and by transferring the data to a PC. We also tried to measure this way the cooling rates obtainable with the sample-filled Al pans used for DSC. However, these rates were much less reproducible, probably because of problems in placing properly the tip of the thermocouple into the sample. Therefore, as pointed out above, for Al pans only an estimate can be given for the cooling rates, which is based on the Leidenfrost effect.

X-ray diffraction curves were recorded in digital form on a PC by means of a voltmeter connected to the *x-y* chart recorder output of the Siemens Kristalloflex instrument and an A/D converter. Measurement time was ~30 min for each diffractogram, which leads to a difference in time scale for the effects seen in the DSC scans on heating at a rate of 30 K min^{-1}. The curves were manipulated by SpectraCalc and smoothed by a Savitzky/Golay 15-point smooth. The temperature of the x-ray camera was regulated with a Paar (Model TTK-HC) temperature controller, and it was constant to ±0.1°. In several of the diffractograms, a change of the instrument's parameters resulted in increased damping and half-band-width. This is seen in Fig. 5 from a comparison of curves 2 and 3 with curves 1 and 4.

After several of the experiments, the UV-visible spectra of the proteins dissolved in phosphate buffer (pH 6.8) were recorded again and found to be indistinguishable from those of the proteins before exposure to the cooling/heating cycles. This is taken as evidence that no irreversible denaturation had occurred.

Heat-denaturated MetHb for Fig. 8 was made by keeping as-received MetHb for 24 h at 378 K. Its insolubility in aqueous phosphate buffer is taken as evidence for irreversible denaturation (Olsen, 1994).

RESULTS

Cooling rate is the most important parameter for complete vitrification of freezable water because, for a given sample size, increasingly higher cooling rates are necessary with increasing hydration of the protein. For the sake of reproducibility of the experiments, we show in Fig. 1 temperature versus time curves that were determined for the sample holders used for the x-ray diffraction studies of the hydrated

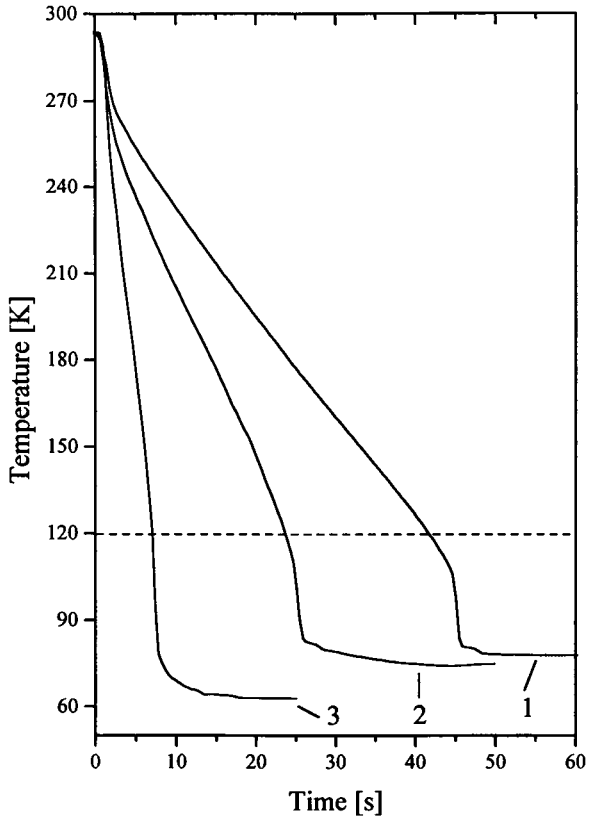

FIGURE 1 Temperature versus time curves for cooling of the sample holders used for x-ray diffraction measurements. Curve 1 is for the original low temperature sample holder dropped in liquid N_2, curve 2 for the same sample holder dropped in N_2 slush. Curve 3 is for the miniature sample holder cooled by dropping it into N_2 slush. For curves 1–3 the average cooling rates for cooling from 293 to 120 K are ~250, ~440, and ~1500 K min^{-1}, respectively. See Materials and Methods for additional details.

protein powders. The broken line is at 120 K, and it denotes the temperature where, according to our previous study (Sartor et al., 1992, 1993), the freezable water should be in the glassy state, well below its glass→liquid transition temperature. Therefore, the evaluation of cooling rates is from 293 to 120 K. Curve 1 is for cooling the original low temperature sample holder by dropping it into liquid N_2; curve 2 is for the same sample holder but with N_2 slush (obtained by pumping on liquid N_2) instead of liquid N_2. The average cooling rates for these two cooling procedures are ~250 and ~440 K min^{-1}. (The rate obtained for procedure 1 is higher than that of ~170 K min^{-1} given in the previous study for the same cooling procedure (Sartor et al., 1992) because that was estimated only by following the Leidenfrost effect.) For curve 3, a much higher cooling rate of ~1500 K min^{-1} was achieved for cooling in N_2 slush by reducing the mass and the thickness of the sample holder. The actual cooling rates of the samples possibly differ from those given here for the sample holders because thermal contact between sample and holder is important. We note that the various quenching techniques give reproducible results in terms of amount of water vitrified. Even higher cooling rates are possible by changing from liquid N_2 and N_2 slush to organic cryomedia (see, e.g., Plattner and Bachmann, 1982), but these cryomedia cannot be pumped off easily and can lead to artifacts both in DSC curves and x-ray diffractograms.

Fig. 2 shows, in the form of x-ray diffractograms recorded at 100 K, the influence of cooling rate on the amount of water vitrified. Curves 1 to 4 are for the same MetHb sample with 0.50 h and cooled at increasing rates of 10, 30, 40, and ~250 K min^{-1}, respectively. This figure clearly shows that, with increasing the cooling rate from 10 to 40 K min^{-1}, the sharp reflections characteristic for hexagonal ice become weaker and, therefore, that the amount of vitrified water must have increased. On cooling at ~250 K min^{-1} (curve 4), sharp bands due to crystalline ice are absent and, therefore, the sample must have been fully vitrified. Curve 4 shows only broad reflections at $2\theta \approx 24°$ and $\approx 40°$. The broad features in this curve must contain contributions from both the vitrified liquid water and the noncrystalline MetHb.

Figs. 3-5 show, in the form of x-ray diffractograms recorded at 100 K, for quenched samples of the three hydrated proteins the range of water content that can be vitrified and its dependence on cooling rate. (The intense reflection at $2\theta \approx 43°$ in several of the diffractograms is from the substrate.) In Fig. 3, curves 1 to 3 are for hydrated MetHb samples with 0.64, 0.66, and 0.73 h, respectively, which were all cooled at ~250 K min^{-1}. Curves 4 and 5 are for hydrated MetHb samples with 0.73 and 0.80 h that were cooled at ~1500 K min^{-1}. Fig. 3 clearly shows that with increasing hydration

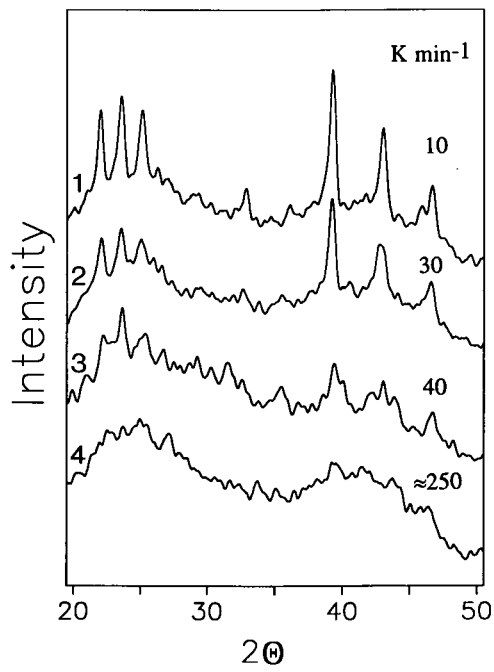

FIGURE 2 X-ray diffractograms (Cu, Kα) of a hydrated MetHb sample with 0.50 h cooled at the rates shown and recorded at 100 K. Note the decreasing intensity of the sharp reflections due to hexagonal ice with increasing cooling rate and their absence in curve 4 (from Sartor et al., 1992).

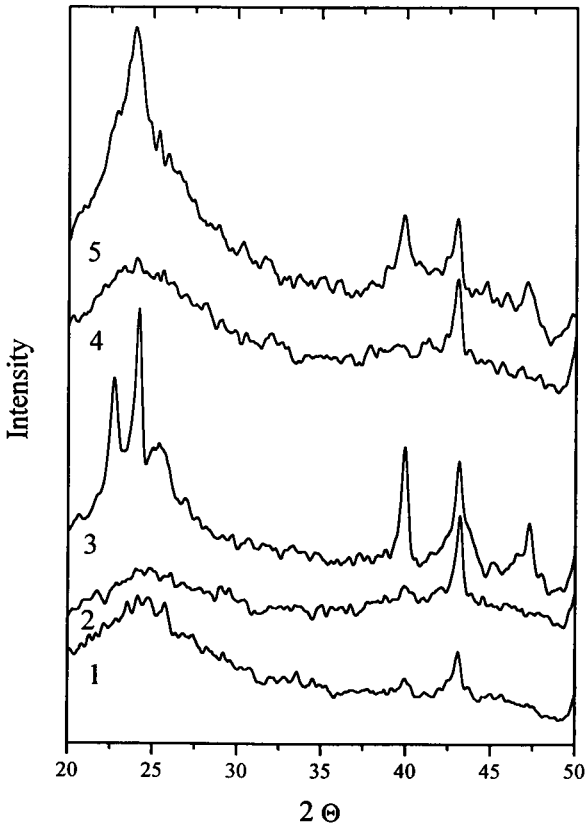

FIGURE 3 X-ray diffractograms (Cu, Kα) of hydrated MetHb samples recorded at 100 K. Curves 1–3 are for samples with 0.64, 0.66 and 0.73 h, respectively, that were cooled at ~250 K min^{-1}. Curves 4 and 5 are for samples with 0.73 and 0.80 h that were cooled at ~1500 K min^{-1}. The intense reflection at $2\theta \approx 43°$ is from the substrate.

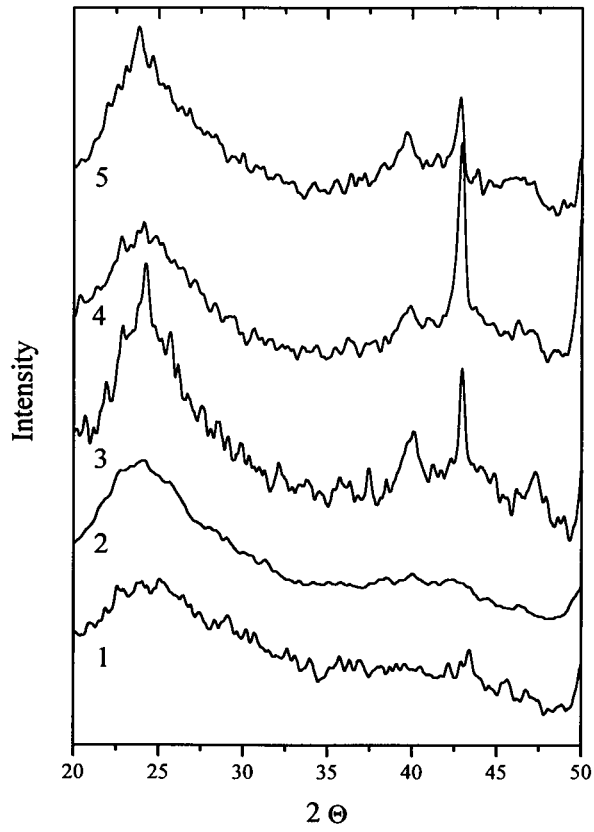

FIGURE 4 X-ray diffractograms (Cu, Kα) of hydrated MetMb samples recorded at 100 K. Curves 1–3 are for samples with 0.54, 0.69, and 0.73 h, respectively, that were cooled at ~250 K min^{-1}. Curves 4 and 5 are for samples with 0.73 and 0.80 h that were cooled at ~1500 K min^{-1}. The intense reflection at $2\theta \sim 43°$ is from the substrate.

an increase in cooling rate is necessary for complete vitrification (e.g., compare curve 3 with curve 4). It further shows by comparison of curve 4 with curve 5 that, for our maximal rate of cooling of ~1500 K min^{-1}, a maximal water content of ~0.73 h can be fully vitrified, whereas for 0.80 h partial formation of ice on quenching is clearly observable in the form of sharp peaks at, e.g., $2\theta \approx 23°$ and $\approx 40°$, which are superimposed on the broad peaks of the amorphous sample.

Similar behavior is observed for hydrated MetMb and lysozyme. In Fig. 4, curves 1 to 3 are for hydrated MetMb samples with 0.54, 0.69, and 0.73 h, respectively, which were all cooled at ~250 K min^{-1}. Curves 4 and 5 are for hydrated MetMb samples with 0.73 and 0.80 h, which were cooled at ~1500 K min^{-1}. In Fig. 5, curves 1 and 2 are for hydrated lysozyme samples with 0.56 and 0.64 h that were cooled at ~250 K min^{-1}. Curves 3 and 4 are for hydrated lysozyme with 0.64 and 0.72 h that were cooled at ~1500 K min^{-1}.

The range of water content that can be fully vitrified by a given cooling rate is very similar for hydrated MetHb and MetMb, but for hydrated lysozyme it is shifted to a lower water content. This is seen by comparing water contents of 0.72–0.73 h; for hydrated MetHb and MetMb samples shown in curves 4 of Figs. 3 and 4, this water content can be fully vitrified by cooling at ~1500 K min^{-1}, whereas for hydrated lysozyme shown in curve 4 of Fig. 5, the same rate of cooling leads to a sample containing crystalline ice. The influence of cooling rate, water content, and type of protein on the amount of vitreous but freezable water shown in the form of the diffractograms of Figs. 3–5 was further analyzed by determining the percentage of the freezable water fraction that could be vitrified. This was done by comparing the areas from the reflections of crystalline ice in diffractograms recorded at 100 K (Figs. 3–5) with those recorded at 240 K where the freezable water fraction has crystallized. These values are collected in Table 1.

Fig. 6 shows the crystallization behavior on reheating a hydrated MetHb sample. Curves 1 and 2 show diffractograms of MetHb samples with 0.50 and 0.70 h that were cooled at ~250 K min^{-1} and recorded at 100 K. Curve 1 shows only two broad peaks; curve 2 shows in addition weakly sharp reflections at, e.g., $2\theta \approx 40°$ that are due to a small amount of crystalline ice. The features of both curves remained unaltered after heating the samples up to 180 K and holding it at this temperature for 30 min. Crystallization of the vitreous but freezable water component in the MetHb sample with 0.70 h (i.e., the sample taken for curve 2)

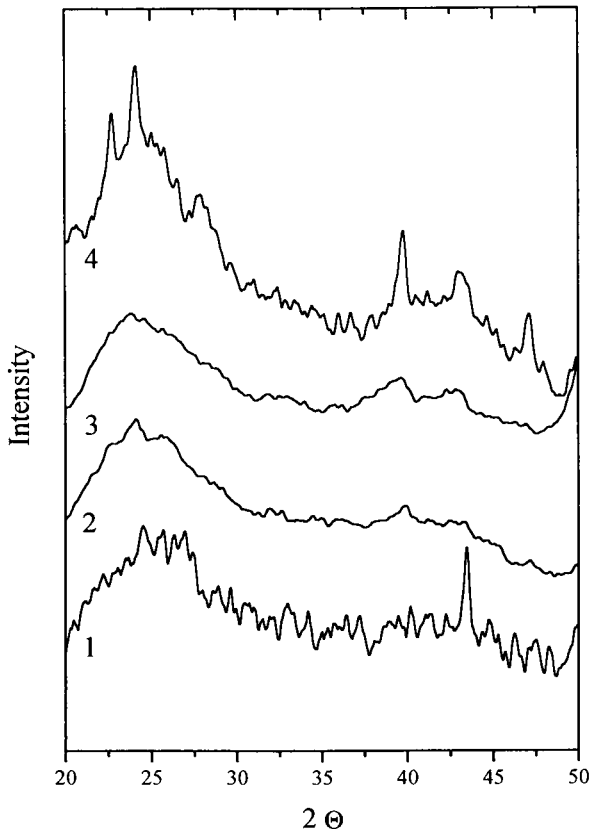

FIGURE 5 X-ray diffractograms (Cu, Kα) of hydrated lsyozyme samples recorded at 100 K. Curves 1 and 2 are for samples with 0.56 and 0.64 h that were cooled at ~250 K min^{-1}. Curves 3 and 4 are for samples with 0.64 and 0.72 h that were cooled at ~1500 K min^{-1}. The intense reflection at $2\theta \approx 43°$ is from the subtrate.

occurred in the temperature region from ~200 to 240 K, as shown in curves 3–5. At 210 K (curve 3), peaks characteristic for cubic ice and marked as Ic started to develop. At 240 K (curve 4), these bands became sharper and more

TABLE 1 Influence of cooling rate, hydration, and protein on the vitrification of the vitreous but freezable water fraction on hydrated MetMb, MetHb, and lysozyme

h (g water/g protein)	Cooling rate (K min^{-1})	% vitrified at 100 K
MetHb: 0.64	~250	100
MetHb: 0.66	~250	100
MetHb: 0.73	~250	16
MetHb: 0.73	~1500	100
MetHb: 0.80	~1500	51
MetMb: 0.54	~250	100
MetMb: 0.69	~250	100
MetMb: 0.73	~250	57
MetMb: 0.73	~1500	100
MetMb: 0.80	~1500	58
Lysozyme: 0.56	~250	100
Lysozyme: 0.64	~250	47
Lysozyme: 0.64	~1500	100
Lysozyme: 0.72	~1500	50

The values are for the diffractograms shown in Figs. 3–5.

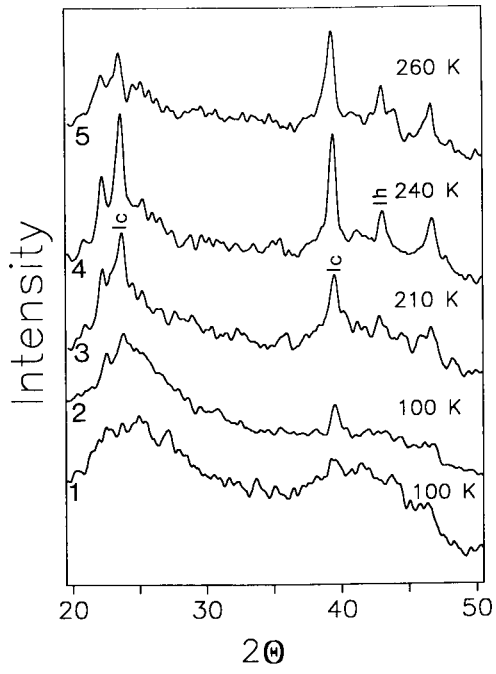

FIGURE 6 X-ray diffractograms (Cu, Kα) of two hydrated MetHb samples (1) with 0.50 and (2) with 0.70 h, both cooled at a rate of ~250 K min^{-1} and recorded at 100 K. Curves 3–5 are diffractograms of the 0.70-h sample taken for curve 2 and heated to and recorded at 210, 240, and 260 K, respectively. Ic and Ih mark some of the reflections of cubic and hexagonal ice. The diffractograms are drawn on the same scale. From Sartor et al., 1992.

intense, and partial conversion to hexagonal ice occurred, as can be seen by the peak at $2\theta \approx 44°$ (marked as Ih). At 260 K (curve 5), further conversion of cubic to hexagonal ice occurred and the ice started to melt.

The calorimetric behavior of the hydrated protein powders observed on reheating quenched samples is shown in Figs. 7-14 in the form of DSC scans. Fig. 7 demonstrates the difference in thermal behavior on reheating between quenched hydrated MetHb containing only vitreous but unfreezable water and those containing in addition vitreous and freezable water. Both samples were cooled at ~150 K min^{-1} and reheated at a rate of 30 K min^{-1}. Curve 1 is a DSC scan of a MetHb sample with 0.30 h, curve 2 the scan of a sample with 0.50 h. In these curves the rising slope indicates strongly increasing heat capacity at ~140–170 K. This increase is superimposed in curve 2 by a broad exotherm centered at ~230 K and a subsequent endotherm. These features are assigned to formation of cubic and hexagonal ice and its melting, in line with the x-ray diffractograms shown in Fig. 6. We note that we have studied recently for hydrated MetHb, MetMb, and lysozyme the increase in heat capacity at ~140–170 K (Sartor et al., 1994) by DSC and attributed it to kinetic unfreezing of molecular motions with an exceptionally broad distribution of relaxation times.

Physical aging, or annealing, of a glass at a temperature below its T_g is known to cause a decrease in enthalpy (and

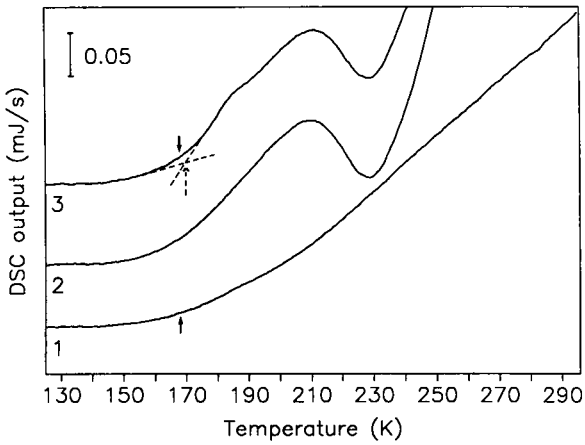

FIGURE 7 Glass→liquid transition at ~169 K and crystallization of hydrated MetHb with 0.50 h, as seen in DSC scans recorded during heating at a rate of 30 K min^{-1}. Curve 2 is obtained after cooling the sample at a rate of ~150 K min^{-1} from 290 to 103 K in the instrument and heating to 295 K. Curve 3 is obtained after cooling the same sample from 295 to 168 K, annealing at 168 K for 90 min, cooling to 103 K, and thereafter reheating. As scan 1 is shown for comparison, the scan of a sample of hydrated MetHb containing only unfreezable water, namely 0.30 h, which has also been cooled at a rate of ~150 K min^{-1}, and annealed at 168 K for 90 min. The broken arrow in curve 3 marks the onset of the glass→liquid transition. General for Figs. 7 to 15: DSC thermograms were recorded only on heating at a rate of 30 K min^{-1}. Solid arrows mark the annealing temperature. The curves are normalized with respect to the samples' weights and are drawn on the same scale but are shifted vertically for clarity. The ordinate scale is for 1 mg sample weight.

entropy and volume) that can be observed in a DSC scan on reheating in form of an overshoot, the size of which is dependent on the temperature and/or time of annealing (Stephens, 1976; Feltz, 1983). The observation of an endothermic step, with an overshoot developing upon annealing, is generally taken as evidence for a glass→liquid transition. We have therefore investigated in detail the influence of various annealing temperatures and times on the DSC scan. Curve 3 in Fig. 7 is the heating curve of the same sample taken for curve 2 and also cooled at ~150 K min^{-1}, which has in addition been annealed at 168 K for 90 min (annealing temperatures marked in this curve and the following figures by the solid arrow). It shows a distinct endothermic step with an onset temperature of 170 K (determined as shown by the broken lines and marked by the broken arrow) and a weak overshoot, which are superimposed on the rising slope. Other annealing temperatures of 171, 163, and 144 K were investigated for the same sample and the same annealing time of 90 min. The endothermic step was less distinct after annealing at 171 or 163 K, and it was not observable after annealing at 144 K. Therefore the annealing conditions used for curve 3 (i.e., at 168 K for 90 min) are used in the following for all samples. It is important to note that in curve 1 identical annealing to that of curve 3 (i.e., 168 K for 90 min) did not give an endothermic step comparable to that of curve 3. This is not in contradiction to our previous study of enthalpy relaxation in hydrated proteins containing only vitreous and unfreezable water (Sartor et al., 1994) because these effects, seen on reheating also in the form of endotherms, are much weaker than those shown by the vitreous but freezable water fraction in curve 3 and in the subsequent figures.

Fig. 8 is the only figure in which a heat-denaturated protein was used for comparison with native protein. Curve 1 is a DSC scan of heat-denaturated MetHb with 0.54 h (from Sartor, 1991); curve 2 is the scan of the same sample but annealed in addition for 90 min at 168 K. Curve 3 is curve 2 expanded 5-fold, and its thermal features are very similar to those of curve 3 of Fig. 7 obtained for native MetHb. Curve 4 was obtained by subtracting curve 1 from curve 2 (10-fold expanded) and it shows development of a characteristic overshoot upon annealing.

Fig. 9 shows for hydrated MetMb samples the influence of physical aging, cooling rate, and water content on the DSC curves recorded for heating at 30 K min^{-1}. Curves 1 and 2 show the influence of physical aging for a MetMb sample with 0.69 h and cooled at ~150 K min^{-1} in the DSC instrument. Curve 1 is for the unannealed sample; curve 2 is for the same sample but annealed at 168 K for 90 min before its heating and recording of its DSC scan. Note the development of a weak endothermic feature upon annealing. Curves 3 and 4 show the influence of cooling rate for another MetMb sample with 0.73 h and annealed at 168 K for 90 min in both cases. The sample was cooled at ~150 K min^{-1} in the DSC instrument for curve 3, but it was cooled at ~1500 K min^{-1} for curve 4. Note in curve 4 the development of an intense endothermic feature with an overshoot, a plateau region and the subsequent intense exotherm. Curves 5 and 6 further show the influence of cooling rate for another MetMb sample with 0.80 h and also annealed at 168 K for 90 min in both cases. The sample was

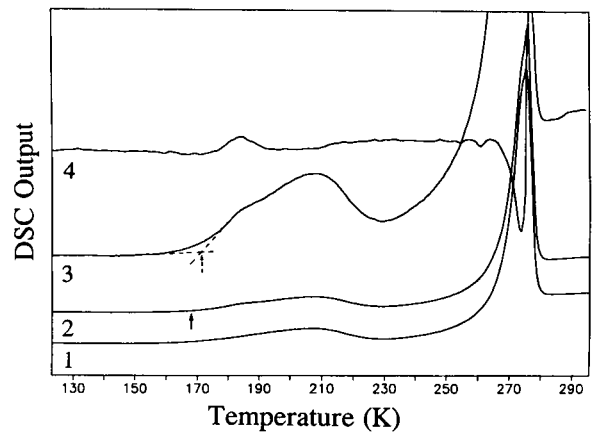

FIGURE 8 Glass→liquid transition at ~169 K and crystallization of heat-denatured MetHb with 0.54 h, as seen in DSC scans recorded on heating. Curve 1 is obtained after cooling the sample from 290 to 103 K at a rate of ~150 K min^{-1} in the instrument; curve 2 is obtained after additional annealing for 90 min at 168 K. Curve 3 is curve 2 expanded 5-fold, the onset of glass→liquid transition marked by the broken arrow. Curve 4 is obtained by subtracting curve 1 from curve 2 and it is shown 10-fold expanded.

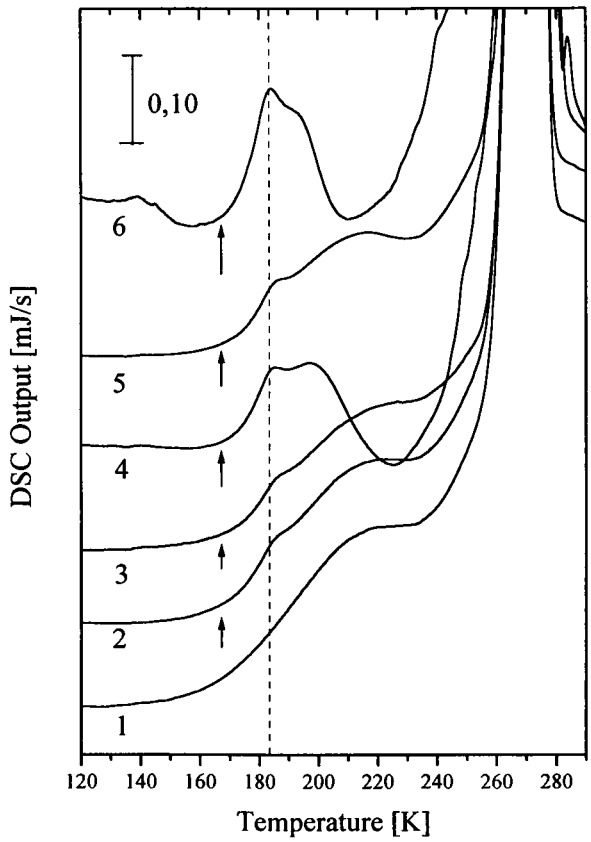

FIGURE 9 Glass→liquid transition at ~171–173 K and crystallization of vitreous water in hydrated MetMb samples as seen in the DSC scans recorded on heating. For curves 2–6 the samples were annealed at 168 K for 90 min before heating and recording its DSC scan; curve 1 is for an unannealed sample. Curves 1 and 2 are for MetMb with 0.69 h that was cooled at ~150 K min^{-1}. Curves 3 and 4 are for MetMb with 0.73 h cooled at ~150 K min^{-1} (curve 3) and ~1500 K min^{-1} (*curve 4*). Curves 5 and 6 are for MetMb with 0.80 h cooled at ~1500 K min^{-1} (*curve 5*) and ~2700 K min^{-1} (*curve 6*).

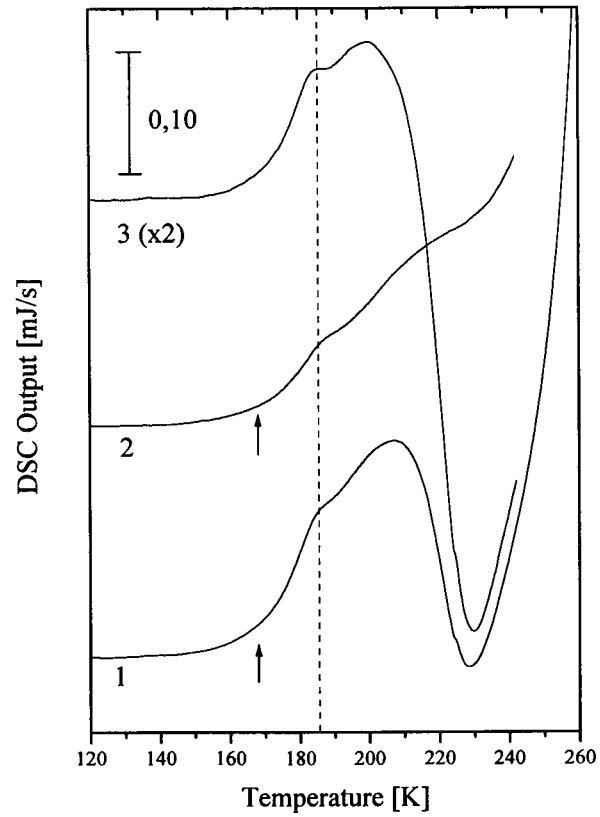

FIGURE 10 Glass→liquid transition at ~170 K and crystallization of vitreous water in hydrated MetMb with 0.54 h as seen in a DSC difference curve. Curve 1 is obtained after cooling the sample from 298 to 103 K at ~150 K min^{-1}, heating the sample to 168 K, annealing it at 168 K for 90 min, cooling it at 30 K min^{-1} to 103 K, and heating it to 298 K and recording its DSC scan. Curve 2 is obtained after cooling the same sample subsequently to 103 K at ~150 K min^{-1}, heating it to 243 K at 30 K min^{-1} for crystallizing the vitreous, but freezable, water fraction, cooling it at ~150 K min^{-1} to 103 K, heating it to 168 K and annealing it at 168 K for 90 min, cooling it to 103 K, and finally heating it to 243 K and recording its DSC scan. Curve 3 is obtained by subtracting curve 2 from curve 1, and it is shown on a twofold enlarged scale.

cooled at ~1500 K min^{-1} for curve 5 and at ~2700 K min^{-1} for curve 6.

The calorimetric features of the vitreous but freezable water fraction are best seen in DSC difference curves. This is shown in Fig. 10 for a MetMb sample with 0.54 h. Curve 1 is for the sample that was cooled at ~150 K min^{-1} and annealed at 168 K for 90 min before its heating and recording of its DSC scan. The treatment for this curve is comparable to that used for curves 2–6 of Fig. 9. For curve 2, the vitreous but freezable water fraction was first crystallized by heating the vitrified sample to 243 K, and the whole procedure was subsequently repeated including annealing at 168 K. Note in curve 2 that the endothermic step at ~185 K and the broad exotherm at ~230 K are very weak in comparison to curve 1. But they are not absent, and we attribute this to incomplete crystallization of the water on heating to 243 K. Curve 3 was obtained by subtracting curve 2 from curve 1, and it is expected to represent on the whole the calorimetric features of the vitreous and freezable water fraction on hydrated MetMb; it shows an endothermic step with a T_g of 170 K and an overshoot and an intense exotherm centered at ~230 K. We are aware that on heating the sample to 243 K for crystallization of this water fraction, changes might have occurred also with the protein's heat capacity and the shape of the melting endotherm of ice that would be contained in the difference curve. Nevertheless, the basic features of the difference curve 3 and of similar difference curves shown below for hydrated MetHb and lysozyme are those of a glass undergoing a glass→liquid transition and crystallization on further heating.

DSC heating curves similar to those for hydrated MetMb are shown in Figs. 11 and 12 for hydrated MetHb powders. Fig. 11 shows the influence of physical aging, cooling rate, and water content on the DSC curves recorded for heating at 30 K min^{-1}. Curves 1 and 2 show the influence of physical aging for a MetHb sample with 0.66 h and cooled at ~150 K min^{-1}. Curve 1 is for the unannealed sample; curve 2 is for the same sample but annealed at 168 K for 90 min before

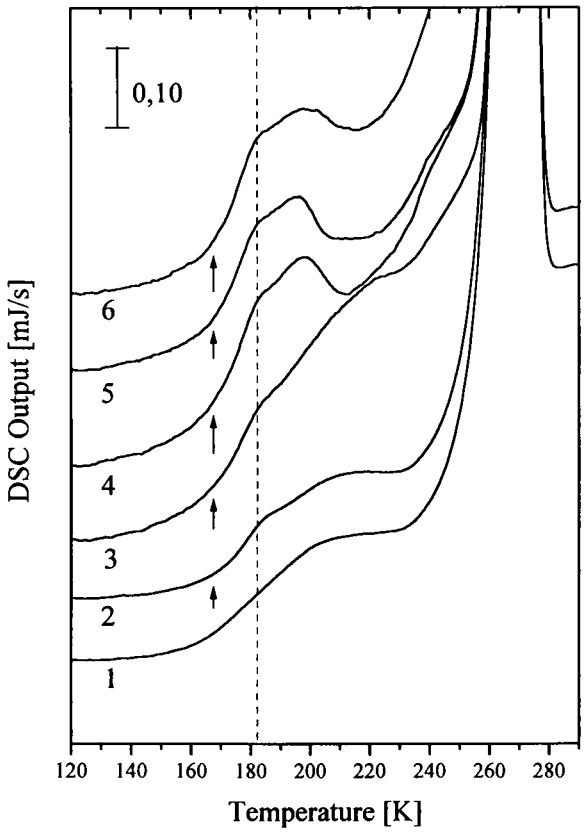

FIGURE 11 Glass→liquid transition at ~166–169 K and crystallization of vitreous water in hydrated MetHb samples as seen in the DSC scans recorded on heating. For curves 2–6 the samples were annealed at 168 K for 90 min before heating and recording its DSC scan; curve 1 is for an unannealed sample. Curves 1 and 2 are for MetHb with 0.66 h that was cooled at ~150 K min^{-1}. Curves 3 and 4 are for MetHb with 0.73 h cooled at ~150 K min^{-1} (*curve 3*) and ~1500 K min^{-1} (*curve 4*). Curves 5 and 6 are for MetHb with 0.80 h cooled at ~1500 K min^{-1} (*curve 5*) and ~2700 K min^{-1} (*curve 6*).

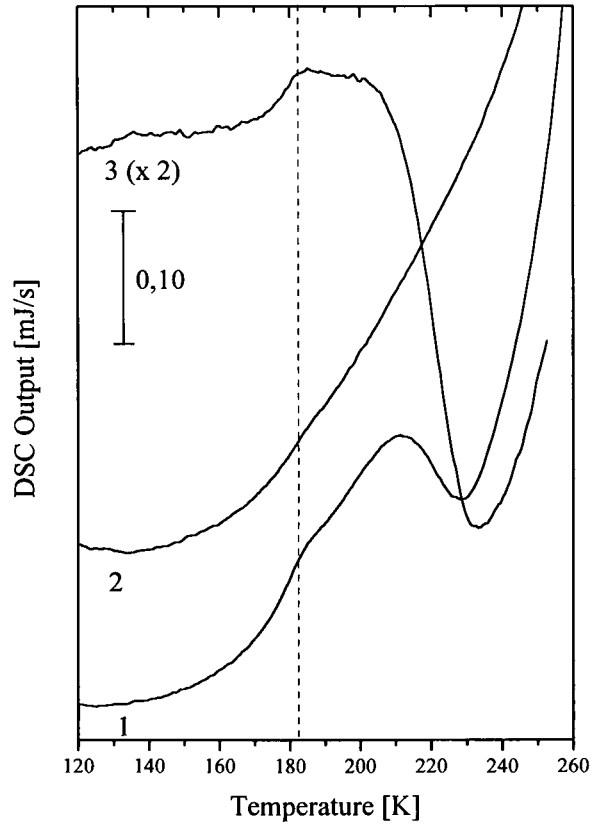

FIGURE 12 Glass→liquid transition at ~171 K and crystallization of vitreous water in hydrated MetHb with 0.50 h as seen in a DSC difference curve. Curve 1 is obtained after cooling the sample from 298 to 103 K at ~150 K min^{-1}, heating the sample to 168 K, annealing it at 168 K for 90 min, cooling it at 30 K min^{-1} to 103 K, and heating it to 298 K and recording its DSC scan. Curve 2 is obtained after cooling the same sample subsequently to 103 K at ~150 K min^{-1}, heating it to 253 K at 30 K min^{-1} for crystallizing the vitreous, but freezable, water fraction, cooling it at ~150 K min^{-1} to 103 K, heating it to 168 K and annealing it at 168 K for 90 min, cooling it to 103 K, and finally heating it to 253 K and recording its DSC scan. Curve 3 is obtained by subtracting curve 2 from curve 1, and it is shown on a twofold enlarged scale.

its heating. Curves 3 and 4 show the influence of cooling rate for another MetHb sample with 0.73 h and annealed at 168 K for 90 min in both cases. The sample was cooled at ~150 K min^{-1} in the DSC instrument for curve 3, but it was cooled at ~1500 K min^{-1} for curve 4. Note in curve 4 the development of an intense endothermic feature with a plateau region and the subsequent exotherm, which is similar to that shown in curve 4 of Fig. 8. Curves 5 and 6 further show the influence of cooling rate for another MetHb sample with 0.80 h and also annealed at 168 K for 90 min in both cases. The sample was cooled at ~1500 K min^{-1} for curve 5 and at ~2700 K min^{-1} for curve 6.

DSC difference curves analogous to that shown in Fig. 10 for hydrated MetMb are shown in Fig. 12 for a MetHb sample with 0.50 h. Curve 1 is for the sample that was cooled at ~150 K min^{-1} and annealed at 168 K for 90 min before its heating and recording of its DSC scan. For curve 2, the vitreous but freezable water fraction was first crystallized by heating the vitrified sample to 253 K, and the whole procedure was subsequently repeated including annealing at 168 K. Note in curve 2 the absence of the endothermic step at ~182 K and of the broad exotherm at ~230 K. Curve 3 was obtained by subtracting curve 2 from curve 1, and it shows, similar to curve 3 of Fig. 9, an endothermic step with an overshoot and a T_g of 171 K. This endothermic step is attributed to the glass→liquid transition of the vitreous but freezable water fraction in hydrated MetMb. It crystallizes on heating above T_g, which is seen in the DSC scan in the form of the broad exotherm with a peak minimal temperature of ~230 K, and it melts on further heating.

The DSC curves for hydrated lysozyme powders are shown in Figs. 13 and 14. Fig. 13 shows the influence of physical aging, cooling rate, and water content on the DSC curves recorded for heating at 30 K min^{-1}. Curves 1 and 2 are for the same lysozyme sample with 0.56 h and cooled at ~150 K min^{-1}, but for curve 2 the sample was in addition annealed at 168 K for 90 min before its heating. Curves 3

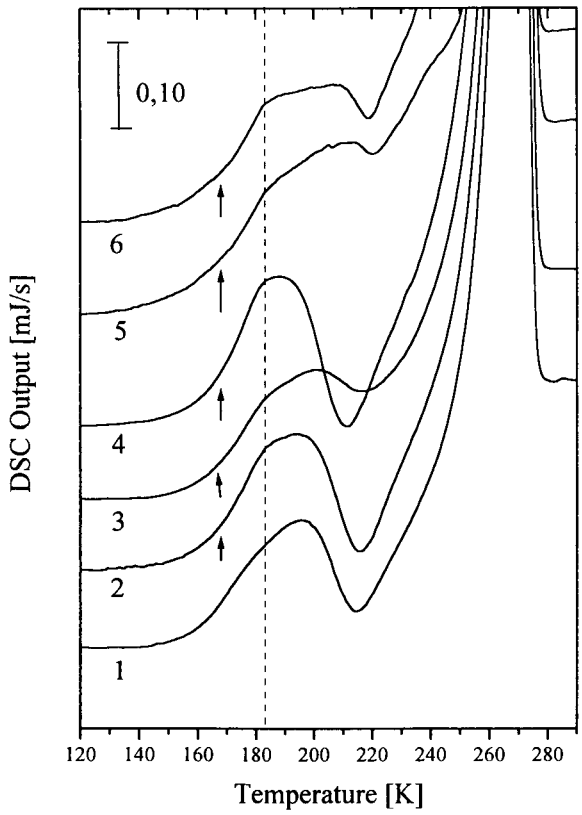

FIGURE 13 Glass→liquid transition at ~164–168 K and crystallization of vitreous water in hydrated lysozyme samples as seen in the DSC scans recorded on heating. For curves 2–6 the samples were annealed at 168 K for 90 min before heating and recording its DSC scan; curve 1 is for an unannealed sample. Curves 1 and 2 are for lysozyme with 0.56 h that was cooled at ~150 K min^{-1}. Curves 3 and 4 are for lysozyme with 0.64 h cooled at ~150 K min^{-1} (*curve 3*) and ~1500 K min^{-1} (*curve 4*). Curves 5 and 6 are for lysozyme with 0.76 h cooled at ~1500 K min^{-1} (*curve 5*) and ~2700 K min^{-1} (*curve 6*).

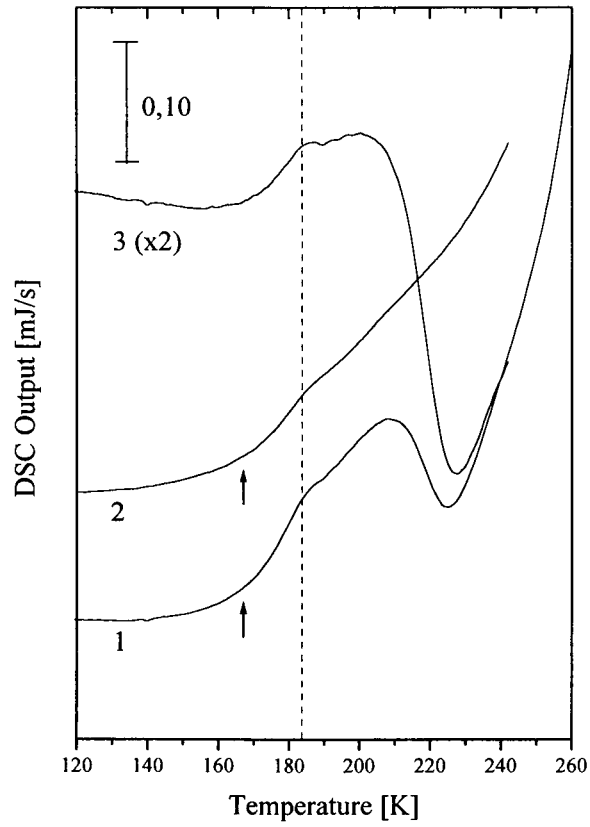

FIGURE 14 Glass→liquid transition at ~168 K and crystallization of vitreous water in hydrated lysozyme with 0.35 h as seen in a DSC difference curve. Curve 1 is obtained after cooling the sample from 298 to 103 K at ~150 K min^{-1}, heating the sample to 168 K, annealing it at 168 K for 90 min, cooling it at 30 K min^{-1} to 103 K, and heating it to 298 K and recording its DSC scan. Curve 2 is obtained after cooling the same sample subsequently to 103 K at ~150 K min^{-1}, heating it to 243 K at 30 K min^{-1} for crystallizing the vitreous, but freezable, water fraction, cooling it at ~150 K min^{-1} to 103 K, heating it to 168 K and annealing it at 168 K for 90 min, cooling it to 103 K, and finally heating it to 243 K and recording its DSC scan. Curve 3 is obtained by subtracting curve 2 from curve 1, and it is shown on a twofold enlarged scale.

and 4 show the influence of cooling rate for another sample with 0.64 h and annealed at 168 K for 90 min in both cases. The sample was cooled at ~150 K min^{-1} in the DSC instrument for curve 3, but it was cooled at ~1500 K min^{-1} for curve 4. Curves 5 and 6 further show for another lysozyme sample with 0.76 h, and also annealed at 168 K for 90 min in both cases, that cooling at ~1500 K min^{-1} (curve 5) or at ~2700 K min^{-1} (curve 6) is not enough for complete vitrification.

DSC difference curves are shown in Fig. 14 for a lysozyme sample with 0.35 h. Curve 1 is for the sample that was cooled at ~150 K min^{-1} and annealed at 168 K for 90 min before its heating and recording of its DSC scan. For curve 2, the vitreous but freezable water fraction was first crystallized by heating the vitrified to sample to 243 K, and the whole procedure was subsequently repeated including annealing at 168 K. Note in curve 2 that the endothermic step at ~182 K and the broad exotherm at ~230 K are very weak in comparison with curve 1, but they are not absent for reasons given above for Fig. 12. Curve 3 was obtained by subtracting curve 2 from curve 1, and it shows, similar to curves 3 of Figs. 10 and 12, an endothermic step with an overshoot and a T_g of 168 K. This endothermic step is attributed to the glass→liquid transition of the vitreous but freezable water fraction in hydrated lysozyme. It crystallizes on heating above T_g, which is seen in the DSC scan in the form of the broad exotherm with a peak minimal temperature of ~230 K, and it melts on further heating.

The original DSC scans of Figs. 9, 11, and 13 show that the endothermic step increases with increasing amount of the vitreous but freezable water fraction. This increase can be seen directly from a comparison of the DSC scans because the scans are normalized for each figure with respect to the samples' weights. The influence of cooling rate on the amount vitrified is best seen by comparing curve 3 in Figs. 9, 11, and 13, in which the samples were cooled at a rate of ~250 K min^{-1}, with those of curve 4 in those figures, in which the same samples were cooled at a 10-fold rate. For determining ΔC_p, the amount of freezable water

causing the endothermic step has to be known. This was determined from the areas of the melting endotherms by using the value of 6.012 kJ mol^{-1} for the heat of melting of bulk ice. For small ice crystal size, this value is expected to be lower, and Handa et al. (1992) have reported for the melting of ice in small pores much lower heats of melting than that of bulk ice at the same temperature (see their Table 1). Small ice crystal size is expected in particular for hydrated protein powders that contain very little freezable water. This was confirmed for hydrated MetHb by the shape and onset temperature of the melting endotherm (Sartor and Mayer, 1994).

Because of these difficulties, ΔC_p values are given in Table 2 for those water-rich protein powders that could be completely vitrified at ~1500 K min^{-1}. These are the MetMb and MetHb samples with 0.73 h and lysozyme with 0.64 h, and their DSC curves are shown as curve 4 in Figs. 9, 11, and 13. X-ray diffractograms of these samples are shown in Figs. 3 and 4 as curve 4 and in Fig. 5 as curve 3, and they confirm that the water is fully vitrified on cooling at ~1500 K min^{-1}. Evaluation of the other DSC scans for ΔC_p also gave values of between ~20 and 40 J K^{-1} (mol of freezable water)$^{-1}$, and this range of ΔC_p values is therefore considered to be characteristic for the vitreous and freezable water fraction. Much higher ΔC_p values were obtained only for samples containing very little freezable water, and this is attributed mainly to the above-mentioned dependence of the heat of melting of ice on ice crystal size.

The range of T_g values obtained for the DSC curves shown in Figs. 7–14 is between ~164 and 174 K and the range of widths between ~9 and 16°.

DISCUSSION

Glass→liquid transition and crystallization behavior of the freezable water fraction is best seen in DSC difference curves that are obtained by subtracting the scan of the sample with the water in the crystallized state from that obtained with the water in the vitreous state. In Fig. 15 the difference curves for hydrated MetMb, lysozyme, and MetHb samples, shown separately as curve 3 in Figs. 10, 12, and 14, are compared here as curves 1–3, and they are further compared in curve 4 with a similar difference curve obtained for the vitreous but freezable water fraction in the pores of PHEMA hydrogel with 0.70 h. The similarity of the four difference curves of the water in natural and synthetic polymers, and the difference from that of glassy bulk water made by hyperquenching of micron-sized droplets shown in Table 2 (Johari et al., 1987; Hallbrucker et al., 1989) indicates that the perturbation of the water structure by the polymer has a common origin that goes beyond the structural details between the four polymers. Therefore the characteristic features of curves 1–4 can be discussed together. This is an important aspect, and because of that we have first shown separately x-ray diffractograms and DSC scans of the three hydrated proteins before comparing them in Fig. 15.

We first give our arguments for an increase in C_p at ~162 K seen in curve 4 of Fig. 15 to glass→liquid transition of

TABLE 2 Calorimetric glass → liquid transition features of vitreous and freezable water on water-rich MetMb, MetHb, and lysozyme and the comparison with those of freezable water in PHEMA hydrogel and of bulk water

Sample	T_g (K)	Width (K)	ΔC_p (J K^{-1} mol^{-1})
MetMb: 0.73 h	172	9	~20
Lysozyme: 0.64 h	162	16	~40
MetHb: 0.73 h	167	13	~23
PHEMA-34*: 0.50 h	163	7	~32
PHEMA-42*: 0.70 h	164	8	~18
Bulk water‡	136 ± 1	~12	1.6 ± 0.1

T_g, width, and ΔC_p refer to the onset temperature, the width, and the increase in heat capacity of the vitreous and freezable water fraction. The DSC scans of the hydrated MetMb, MetHb and lysozyme samples are shown as curve 4 of Figs. 9, 11, and 13.

*Values are from Hofer et al. (1990) and Sartor et al. (1992).

‡The values are from Johari et al. (1990).

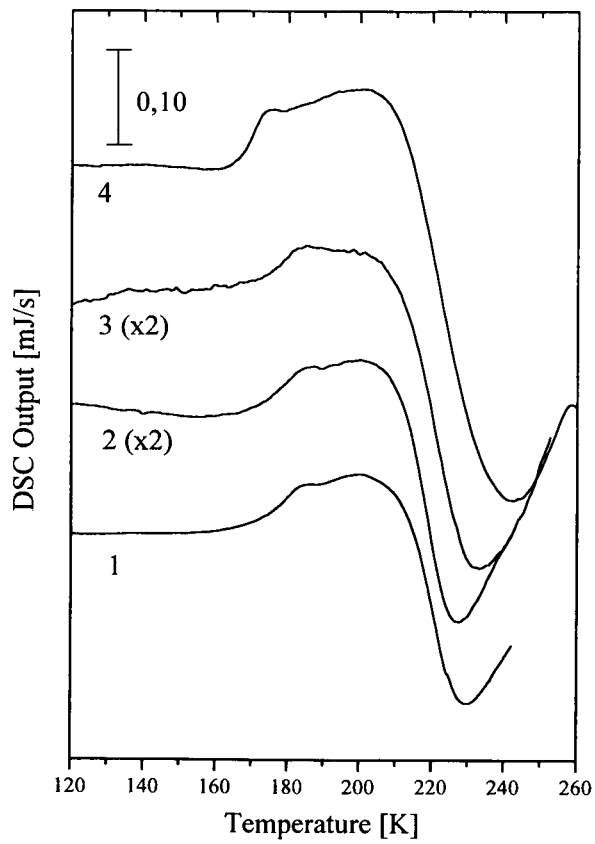

FIGURE 15 DSC difference curves obtained by subtracting the DSC scan where the water fraction has been crystallized from that of the vitreous water fraction. Curve 1 is for MetMb with 0.54 h, curve 2 for lysozyme with 0.35 h, and curve 3 for MetHb with 0.50 h. Curve 4 is for a PHEMA-42 hydrogel sample containing ~41% water (i.e., 0.70 h), and it was obtained by subtracting curve 5 from curve 4 in Fig. 1 of Hofer et al. (1990). Curves 1, 2, and 3 are the curves shown as curves 3 in Figs. 10, 14, and 12 (see Table 2).

mainly vitreous and freezable water in PHEMA hydrogel because relevant low temperature studies have been made for this system; we then proceed to the proteins. (1) The increase in C_p at 162 ± 2 K is not affected by the difference in the cross-linking densities between different PHEMAs and therefore it is mainly associated with the water fraction (Hofer et al., 1990). If the T_g would be due mainly to the polymer's network, then a change in cross-linking density should cause a change in T_g value (Mark et al., 1993). (2) For D_2O in PHEMA hydrogel, the increase in C_p is shifted by ~3 K to higher temperature in comparison with H_2O (Hofer et al., 1990). This is the shift expected for isotopic substitution of H_2O by D_2O (Johari et al., 1990). (3) NMR spectroscopy of water-rich PHEMA hydrogel by Smyth et al. (1988) shows that water becomes mobile at ~180 K and freezes on heating between 230 and 260 K, which is consistent with the assignment given above. (4) Development of an overshoot on physical aging below T_g is a characteristic of glass→liquid transition and such an overshoot was observed for water-rich PHEMA hydrogels (Hofer et al., 1990, 1992) for hydrated MetHb (Sartor et al., 1992) and in this study. (5) The endothermic steps at ~160–170 K disappear on heating and crystallizing the vitreous and freezable water fraction. This is the behavior expected for heating a glass above its glass→liquid transition region, and it has been demonstrated for water in PHEMA hydrogel (Hofer et al., 1990) and for water on hydrated MetHb (Sartor et al., 1992, 1993), and it is shown further in this study in Figs. 10, 12, and 14. Corkhill et al. (1987) suggest in a simplistic view of the water-binding process in hydrogels "that in non-freezing water the water molecules are hydrogen bonded to hydrophilic groups on the polymer chain, while freezing water molecules are hydrogen bonded to both freezing and non-freezing water molecules". This view allows for dynamical modification of freezable water by interaction with the macromolecule's hydrophilic groups via the unfreezable water and conversely for plasticization of the macromolecule's segments by the freezable water.

The same assignment is used for the hydrated proteins and increase in C_p seen between ~164 and 174 K in the DSC scans of Figs. 7–14 and, more clearly in the difference curves 1–3 of Fig 15, is also attributed to the glass→liquid transition that is mainly associated with the vitreous and freezable water fraction and not with the protein's segments. This water fraction is both structurally and dynamically modified by hydrophilic and H-bonded interaction with the proteins' functional groups via the unfreezable water, and conversely it can exert a plasticizing effect on the proteins' segments. This interaction does not require the tertiary structure of a native protein because DSC scans of heat-denaturated and native MetHb samples show similar thermal features (see Figs. 7 and 8). Similar behavior was also observed for native and heat-denaturated lysozyme (Sartor, 1991; not shown here) and for native and heat-denaturated cytochrome *c* (Fig. 2 in Green et al., 1994).

Green et al. (1994) recently presented a different assignment for the endothermic steps at ~160–170 K seen in DSC scans of hydrated MetHb powders (Sartor, 1991, 1994; Sartor et al., 1992, 1993), of water-rich PHEMA hydrogels (Hofer et al., 1990, 1992), and in their own study of hydrated cytochrome *c* and Mb powders (Green et al., 1994) in terms of onset of a strong water-sensitized β-relaxation, apparently caused by the protein's side chain rotations. Generally speaking, mobility in the glassy state at $T \ll T_g$ is attributed to secondary, or β-, relaxation, whereas the main, or α-relaxation causes the glass→liquid transition (Johari and Goldstein, 1970; for review see Johari, 1987). We reject the assignment of the endothermic steps at ~160–170 K to β-relaxation by Green et al. (1994) and prefer ours in terms of glass→liquid transition of the vitreous and freezable water fraction for the reasons given above and the following additional reasons. (1) The height of a β-relaxation peak decreases upon physical aging in both dielectric and mechanical measurements (Johari, 1987). The calorimetric effect of physical aging on β-relaxation would be a decrease of the height of the endotherm. However, we observe development of an overshoot as an effect of physical aging, which is a characteristic feature of glass→liquid transition. (2) The ΔC_p value at T_g of ~20–40 J K^{-1} (mol of freezable water)$^{-1}$ is similar to those observed for highly concentrated aqueous solution glasses (Angell and Tucker, 1980). Much lower values for changes in heat capacity are observed for β-relaxation than for α-relaxation, as pointed out by Fan et al. (1994). We further note that the experimental evidence for a similar increase in heat capacity in the β- and α-relaxation region reported by Fan et al. (1994) so far is only speculative.

We next discuss in a phenomenological way the calorimetric features of the vitreous and freezable water fraction, seen most clearly in the DSC subtraction curves of Fig. 15, and their difference to those of glassy bulk water (see Table 2) with respect to (1) the T_g value, (2) ΔC_p, and (3) the crystallization behavior.

1. T_g is the temperature at which configurational degrees of freedom become thermally activated and detectable in the C_p during the heating of a glass at a certain rate, as its viscosity decreases to a value near 10^{13} P. As materials at their calorimetric T_gs are considered to be in an isoviscous or isorelaxational state of shear viscosity of ~10^{13} P (Kauzmann, 1948; Feltz, 1983), the increase in T_g values from 136 K for glassy bulk water (Johari et al., 1987, Hallbrucker et al., 1989) to ~170 K for vitreous but freezable water in hydrated proteins implies that for a given temperature, say 136 K, the viscosity is much higher or the relaxation time much longer for the vitreous and freezable water fraction in proteins than for glassy bulk water. The magnitude of the difference in viscosity at a given temperature between glassy bulk water and the vitreous but freezable water fraction in proteins depends on whether the viscosity has a temperature dependence according to Arrhenius or to Vogel-Tammann-Fulcher that is not known (Johari et al., 1990; Angell, 1993). But in either case the viscosity of the vitreous and freezable water fraction must be several orders of magnitude higher than that of bulk water at the same tem-

perature, and it is an indication for both structural and dynamical perturbation of water's H-bonded network by the protein. Dynamical measurements as done here cannot provide details on the type of perturbation, but we note that Jeffrey and Saenger (1994) anticipate from neutron diffraction studies that "three-center hydrogen bonding is of major importance in the description of dynamical processes occurring during hydration of biological macromolecules." This holds not only for water H-bonding directly with, e.g., a protein's functional groups but also for water interacting with a protein's surface via a second water molecule. An increase in T_g is consistent with our estimate of ~55 kJ mol^{-1} for the activation enthalpy of glassy bulk water near T_g (Johari et al., 1987; Hallbrucker et al., 1989) and a value twice as large for water in PHEMA determined from the heating rate dependence of its T_g at ~162 K (Hofer et al., 1990, 1992). It is, furthermore, consistent with measurements of water diffusion coefficients on proteins reported by Kotitschke et al. (1990, Fig. 4); for the same hydration range of ~0.4–0.7 h studied here, at 298 K, diffusion coefficients of water on the protein are lower than that of bulk water by a factor of ~5–10.

2. ΔC_p values at T_g are on the whole independent of heating rate, and they are characteristic for a material and are used in that way (see, e.g., Kauzmann, 1948; Wunderlich, 1960; Wong and Angell, 1976; Moynihan et al., 1976; Johari, 1993). Therefore, the increase in ΔC_p by more than an order of magnitude in going from glassy bulk water to that observed for the vitreous but freezable water fraction in the hydrated proteins, and similar ΔC_p value for freezable water in the synthetic hydrogel PHEMA, is significant (see Table 2). The ΔC_p value for glassy bulk water made by hyperquenching of the liquid is 1.6 J K^{-1} mol^{-1} (Hallbrucker et al., 1989; Johari et al., 1990; Mayer, 1994a). The magnitude of ΔC_p at T_g indicates primarily a contribution from configurational changes as diffusion of molecules becomes probable on the calorimetric time scale, with structural relaxation times of ~70 s at T_g for heating at 30 K min^{-1} (Angell and Torrell, 1983), and the liquid-like degrees of freedom become accessible. For tetrahedrally bonded networks such as GeO_2, SiO_2, BeF_2, etc., the various configurations of the network in the glassy and liquid state of the glass→liquid transition region are entropically not much different from each other and, therefore, these glasses show an extremely small ΔC_p at their respective T_gs (Wong and Angell, 1976). The low value of ΔC_p of 1.6 J K^{-1} mol^{-1} at T_g of hyperquenched glassy water has also been suggested to be a reflection of similar tetrahedrally bonded structures (Hallbrucker et al., 1989; Hofer et al., 1990), which is consistent with diffraction measurements (Hallbrucker et al., 1991; Bellissent-Funel et al., 1992). The much higher value of ΔC_p at T_g of ~170 K in the glass→liquid transition region of the vitreous but freezable water in the hydrated proteins, and similarly in the PHEMA hydrogel, therefore implies structural changes. This is not surprising as H bonding with hydrophilic groups of the polymer networks, e.g., via three-centered hydrogen bonds mentioned above, would substantially affect both the energy of breaking and reforming a H bond and of rotation about an O—H···O bond. ΔC_p values similar to those of the freezable water fraction in the proteins are obtained for concentrated aqueous solution glasses (Angell and Tucker, 1980).

3. The state of liquid water in the hydrated proteins is stable up to ~180 K for 30 min or for shorter times even up to ~200 K when heated at 30 K min^{-1} (Fig. 15), and it begins to transform slowly into cubic ice at ~210 K (see curve 3 of Fig. 6). Therefore, nucleation and crystal growth to form cubic ice occurs at ~50 K higher temperature than in hyperquenched glassy bulk water. Even after crystallization has begun, the amount of cubic ice formed is initially less and it increases with a further increase in temperature to 240 K. A catastrophic crystallization such as that of glassy bulk water (Johari et al., 1987, 1990; Hallbrucker et al., 1989; Hage et al., 1994) clearly does not occur for freezable water on the hydrated proteins. For the MetHb sample shown in Fig. 6, conversion of cubic to hexagonal ice is not complete even at 260 K (curve 5). The DSC difference curves in Fig. 15 also show that the intense exotherm attributed to crystallization of the water fraction is very broad. Its width cannot be determined accurately because on further heating the intense endotherm due to the melting of ice overlaps with the broad exotherm, but it is estimated to go from ~200 to ~250 K. We note that the exothermic contribution from the cubic to hexagonal ice phase transition would not be observable here because of its small value of −50 J mol^{-1} (Handa et al., 1986). The crystallization behavior depends somewhat on the protein and its hydration and on the time scale of the experiment. In particular, for hydrated lysozyme samples, crystallization was observed to occur for the same water content at a lower temperature than for MetHb or MetMb samples.

We next discuss the hydration range of freezable water in the three proteins that can be fully vitrified with the cooling rates used in this study. This is seen best in the x-ray diffractograms shown in Figs. 3–5. With the highest cooling rate of ~1500 K min^{-1}, hydrated MetMb and MetHb samples with 0.73 h can be fully vitrified whereas for samples with 0.80 h formation of ice is observed (see Figs. 3 and 4, curves 4 and 5, and Table 1). For hydrated lysozyme samples, the water content vitrifiable with the same cooling rate is lower by ~0.1 h than those of hydrated MetHb and MetMb (see Fig. 5, curves 3 and 4, and Table 1). This goes parallel with a lower value of unfreezable water of ~0.30 h for lysozyme in comparison with those of ~0.40 h for MetHb and MetMb reported in the literature (see, e.g., Kuntz and Kauzmann, 1974, Table XXI; Doster et al., 1986; Poole et al., 1987), and it was also observed by us.

The DSC curves recorded on heating the quenched samples also show the influence of cooling rate and water content (see Figs. 9, 11, and 13). But here the calorimetric features are not as easily interpreted as the x-ray diffractograms, and it requires a combination of both techniques for full understanding. For example, curve 4 of Fig. 9 nicely shows for a MetMb sample with 0.73 h and quenched at

$\sim$1500 K min^{-1} a glass→liquid transition endotherm with an overshoot and an intense broad exotherm due to crystallization. In curve 5, however, in which a MetMb sample with a slightly higher water content of 0.80 h was quenched at the same rate of $\sim$1500 K min^{-1}, the calorimetric features are not as clearly separable as in curve 4, and it requires for the same sample a higher cooling rate of $\sim$2700 K min^{-1} to be able to observe clearly in curve 6 the several calorimetric features. This has obviously to do with formation of ice on cooling the sample for curve 5, which then on reheating alters the rate of crystallization of the freezable water fraction. Similar behavior can be seen in Figs. 11 and 13.

With a further increase in cooling rate, beyond the value of $\sim$1500 K min^{-1} used here for the x-ray diffraction studies or of $\sim$2700 K min^{-1} for DSC, obviously additional layers of water can be vitrified until the cooling rates approach those of $\sim 10^6$ to 10^7 K s^{-1}, which are necessary for complete vitrification of micron-sized droplets of dilute aqueous solutions and of pure liquid water (Bald, 1986; Bachmann and Mayer, 1987; Mayer and Astl, 1992; Mayer, 1994a,c). It is obvious that with increasing dilution increasing cooling rates are necessary for complete vitrification and that the glass→liquid transition features approach those reported for dilute aqueous solutions (Hofer et al., 1989, 1991) and eventually for pure liquid water (Johari et al., 1987, 1990; Hallbrucker et al., 1989). But, it is important to know whether this increase in cooling rate necessary for vitrification is continuous or abrupt. For MetMb and MetHb, the minimal cooling rate required for complete vitrification of the water fraction increases drastically in going from $\sim$0.7 to $\sim$0.8 h, whereas for lysozyme a similar drastic increase is observed in going from $\sim$0.6 to $\sim$0.7 h. This is indicated in Figs. 3–5 and in Table 1 by an abrupt increase in cooling rate necessary for complete vitrification; whereas MetMb and MetHb samples with water content up to $\sim$0.7 h or lysozyme up to $\sim$0.6 h can be completely vitrified with a rate of $\sim$250 K min^{-1}, it is not possible to fully vitrify samples with only an additional increase in h of $\sim$0.1 even with a sixfold higher rate of $\sim$1500 K min^{-1}. Furthermore, the amount of ice formed in these samples corresponds not to that additional $\sim$0.1 h but is much more; it is $\sim$50% of the freezable water fraction (Table 1).

The concept of a minimal or critical cooling rate, R_c, required for vitrification of a liquid was developed by Uhlmann (1972; Uhlmann and Yinnon, 1983). A maximum in the of rate of crystallization at a temperature, T_n, arises because of the competition between the driving force for crystallization, which increases with increasing supercooling, and the molecular mobility, which decreases with increasing supercooling. Because of that maximum it is possible to estimate from R_c the time τ_n the liquid spends at the temperature T_n before it crystallizes. This time then can be taken as an indicator for the mobility of the liquid at this temperature T_n. In a first-approximation approach, $R_c \approx \Delta T_n/\tau_n$, where ΔT_n is $T_m - T_n$. This relationship allows us to obtain from the R_c values an estimate for τ_n. We do not know T_n on cooling bulk water, but even so, a comparison of τ_n values is meaningful because the R_c values for bulk water and for the freezable water fraction differ by five to six orders of magnitude. R_c for bulk water has been estimated (Bachmann and Mayer, 1987; Mayer, 1994a,c) and calculated (Bald, 1986) as $\sim 10^6$-10^7 K s^{-1}, and R_c for the freezable water fraction in hydrated proteins for water content up to $\sim$0.7 h for MetMb or MetHb, or $\sim$0.6 h for lysozyme as $\sim$25 K s^{-1} (i.e., $\sim$1500 K min^{-1}). For a ΔT_n of $\sim$50°C, this then gives for τ_n of bulk water $\sim 10^{-4}$-10^{-5} s, and for τ_n of the freezable water fraction $\sim$2 s. This difference between the two τ_n values emphasizes the difference in mobility between bulk water and the freezable water fraction at T_n.

The observation of a drastic increase of R_c in the hydration region of between $\sim$0.7 and 0.8 h for MetHb or MetMb and $\sim$0.6 and 0.7 h for lysozyme might be related to reports by Kimmich and co-workers (Kimmich et al., 1990; Kotitschke et al., 1990; Kimmich, 1993) on a threshold water content in the hydrated protein bovine serum albumin (BSA) at $\sim$0.75 h (i.e., $\sim$43 wt%). Kimmich et al. (1990) show in their Fig. 7 the concentration dependences of the water diffusion coefficient in BSA solution at three temperatures. The threshold at $\sim$0.75 h is seen in the form of an abrupt increase of the water diffusion coefficient in going from concentrated to dilute solution. The abrupt increase of diffusion at the threshold hydration is attributed to a percolation transition of clusters of free water, and it indicates the hydration value where the percolation clusters of the free water change from the "finite" regime, with only "islands" of free water, to the "infinite-cluster-regime." The threshold value is remarkably close to the hydration region where a drastic increase in minimal cooling rate is necessary for complete vitrification, and the abrupt increase in the water diffusion coefficient is consistent with an abrupt increase in R_c. Kimmich et al. (1990) point out that the threshold value is well above that of the first hydration layer. However, the hydration range for both the threshold value of water's diffusion coefficient and the abrupt increase in R_c is close to that necessary for completing the secondary hydration shell. We surmise that in the vitreous but freezable water fraction we observe water of the secondary hydration shell and that its calorimetric features are those characteristic for structural and dynamical perturbation of water's H-bonded network by interaction with a protein's surface. Arguments for and against a secondary hydration shell on proteins are summarized by Lounnas et al. (1994).

In our previous study of freezable water on hydrated MetHb (Sartor et al., 1992, 1993) we had preferred its assignment to water in pores and/or loops of the protein's chains because of the similarity with water in the pores of a PHEMA hydrogel, with pores of <30 Å diameter (Bosio et al., 1992). We now prefer the assignment in terms of a secondary hydration shell because of new experimental evidence in the form of similar behavior for the three proteins, of an abrupt increase in critical cooling rate at a hydration value where the secondary hydration shell is

expected to be completed, and of the remarkable similarity of this hydration value to that of the threshold value for water on hydrated BSA (Kimmich et al., 1990). The secondary hydration shell is not expected to be uniformly distributed on the protein, and evidence for clustering of the water has been reported (see, e.g., Doster et al., 1986; Goldanskii and Krupyanskii, 1989; Kimmich et al., 1990; Kotitschke et al., 1990; Kimmich, 1993). The vitreous and freezable water embedded in the pores of a PHEMA hydrogel can then also be seen as clusters of water, although probably of larger size, which are structurally and dynamically modified in comparison with bulk water by interaction with the macromolecule's hydrophilic groups, and the similarity of its calorimetric features to those of the water on the proteins can be understood this way.

The calorimetric features of the vitreous but freezable water fraction on the hydrated proteins cannot be due to the secondary hydration shell alone but must also involve some of the water of the primary hydration shell. This is seen most clearly in curve 2 of Fig. 15 where the DSC difference curve of a lysozyme sample with 0.35 h is shown, with calorimetric features similar to those of samples with much higher water content. The hydration of 0.35 h used for curve 2 is lower than that of 0.38 h necessary for completion of the primary hydration shell of lysozyme (Rupley and Careri, 1991). This observation is consistent with Kimmich et al. (1990, see Fig. 7) who report that no abrupt change is observable in water's diffusion coefficient in the hydration range where the primary hydration shell is completed.

Perturbation of the properties of second-layer water by the protein is estimated to be lower by approximately an order of magnitude than that of the first layer (Rupley and Careri, 1991, Table 7). Apparently because of that, it is not seen in heat capacity measurements of hydrated lysozyme (Yang and Rupley, 1979; Rupley et al., 1983; Rupley and Careri, 1991). We conclude that calorimetric studies of the glass→liquid transition region are more sensitive to small structural and dynamical details and deviations from water's bulk properties than studies of, e.g., heat capacity at ambient temperature. Dynamical measurements on hydrated proteins also indicate perturbation of the water structure beyond the primary hydration shell (Kuntz and Kauzmann, 1974; Rupley and Careri, 1991). However, in these studies done in general at ambient temperature, rapid exchange with bulk water occurs and a time-averaged signal is obtained. Studies of the glass→liquid transition region apparently can have advantages over dynamical measurements at ambient temperature because at low temperatures the relaxation time scales of bulk water and water on the protein can be separated sufficiently to observe their distinct glass→liquid transitions.

For lysozyme, Rupley et al. (1983) have shown in their Fig. 1 that its enzymatic activity increases with increasing hydration for the range of 0.2 to 0.9 h. The range of the vitreous but freezable water fraction characterized here for hydrated lysozyme is within the range where enzymatic activity increases with hydration, and it is suggestive of the importance of this water fraction for the protein's function. Rupley et al. (1983) state that "although multi-layer water is not important for time-average behavior, it is for some dynamic properties." The glass→liquid transition and crystallization behavior of the vitreous but freezable water fractions of the three proteins reported here and its difference from that of bulk water is primarily of dynamic origin. But, this large difference between bulk water and the freezable water fraction must also involve a difference in their structure.

Finally, we address the question of whether or not during vitrification of the vitreous but freezable water fraction by rapid cooling the water molecules occupy the same positions at ambient and at cryogenic temperatures or whether clustering of the water molecules occurs during cooling. This question is of general importance for any attempt to use measurements taken at subzero temperatures for interpreting the behavior at ambient temperature, and it has been argued that this approach might not necessarily be meaningful (Kuntz and Kauzmann, 1974; Rupley and Careri, 1991). We expect that clustering of water during cooling depends primarily on the cooling rate and the degree of hydration and that it is favored by decreasing the cooling rate and increasing the hydration. In our recent study of crystal growth of ice on hydrated MetHb (Sartor and Mayer, 1994), which was followed by comparison of melting endotherms, we surmised that for the hydration range of up to $\sim$0.50 h cooled at rates of $\geq$150 K min^{-1}, the distribution of water molecules present at ambient temperature on the whole does not change. This is consistent with Teeter's (1991) observation that for crystals of the protein crambin "flash-cooled" to 130 K, many of the water positions at 130 K correspond almost exactly with what is seen at 300 K. Therefore the calorimetric features shown, for example, in Fig. 15 are likely those of the vitrified but freezable water fraction with a distribution similar to that at ambient temperature.

Financial support by the Forschungsförderungsfonds of Austria (project P10404-PHY) is acknowledged.

REFERENCES

Angell, C. A. 1993. Water II is a "strong" liquid. *J. Phys. Chem.* 97: 6339–6341.

Angell, C. A., and L. M. Torrell. 1983. Short time structural relaxation in liquids: comparison of experimental and computer simulation glass transitions on picosecond time scales. *J. Chem. Phys.* 78:937–945.

Angell, C. A., and J. C. Tucker. 1980. Heat capacity changes in glass-forming aqueous solutions and the glass transition in vitreous water. *J. Phys. Chem.* 84:268–272.

Bachmann, L., and E. Mayer. 1987. Physics of water and ice: implications for cryofixation. *In* Cryotechniques in Biological Electron Microscopy. R. A. Steinbrecht and K. Zierold, editors. Springer Verlag, Berlin. 1–34.

Bald, W. B. 1986. On crystal size and cooling rate. *J. Microsc.* 143: 89–102.

Barkalov, I. M., A. I. Bolshakov, V. I. Goldanskii, and Yu F. Krupyanskii. 1993. Vitrification effects in water-protein systems. *Chem. Phys. Lett.* 208:1–4.

Bellissent-Funel, M. C., L. Bosio, A. Hallbrucker, E. Mayer, and R. Sridi-Dorbez. 1992. X-ray and neutron scattering studies of the structure of hyperquenched glassy water. *J. Chem. Phys.* 97:1282–1286.

Bosio, L., G. P. Johari, M. Oumezzine, and J. Teixeira. 1992. X-ray and neutron scattering studies of the structure of water in a hydrogel. *Chem. Phys. Lett.* 188:113–118.

Champion, P. M. 1992. Raman and kinetic studies of myoglobin structure and dynamics. *J. Raman Spectrosc.* 23:557–567.

Cooke, R., and I. D. Kuntz. 1974. The properties of water in biological systems. *Annu. Rev. Biophys. Bioeng.* 3:95–125.

Corkhill, P. H., A. M. Jolly, C. O. Ng, and B. J. Tighe. 1987. Synthetic hydrogels. I. Hydroxyalkyl acrylate and methacrylate copolymers: water binding studies. *Polymer.* 28:1758–1766.

Czybulka, U., D. Thoenes, W. Nocker, H. Engelhardt, and A. Mayer. 1993. Thermal properties of the protein-water system at low temperature. *In* Water-Biomolecule Interactions, Conference Proceedings, Vol. 43. M. U. Palma, M. B. Palma-Vittorelli and F. Parak, editors. SIF, Bologna. 139–142.

Doster, W., A. Bachleitner, R. Dunau, M. Hiebl, and E. Lüscher. 1986. Thermal properties of water in myoglobin crystals and solutions at subzero temperatures. *Biophys. J.* 50:213–219.

Doster, W., Cusack, S., and Petry, W. 1989. Dynamical transition of myoglobin revealed by inelastic neutron scattering. *Nature.* 337: 754–756.

Doster, W., S. Cusack, and W. Petry. 1990. Dynamic instability of liquid-like motions in a globular protein observed by inelastic neutron scattering. *Phys. Rev. Lett.* 65:1080–1084.

Doster, W., S. Cusack, and W. Petry. 1991. Structural dynamics of proteins, scaling behaviour and liquid glass transition. *J. Non-Crystall. Solids.* 131–133:357–361.

Doster, W., T. Kleinert, F. Post, and M. Settles. 1993. Effect of solvent on protein internal dynamics: the kinetics of ligand binding to myoglobin. *In* Protein-Solvent Interactions. R. B. Gregory, editor. M. Dekker, New York.

Fan, J., E. I. Cooper, and C. A. Angell. 1994. Glasses with strong calorimetric β-glass transitions and the relation to the protein glass transition problem. *J. Phys. Chem.* 98:9345–9349.

Feltz, A. 1983. Amorphe und Glasartige Anorganische Festkörper. Akademie-Verlag, Berlin. 51.

Frauenfelder, H., and E. Gratton. 1986. Protein dynamics and hydration. *Methods Enzymol.* 127:207–216.

Goldanskii, V. I., and Y. F. Krupyanskii. 1989. Protein and protein-bound water dynamics studied by Rayleigh scattering of Mössbauer radiation. *Quart. Rev. Biophys.* 22:39–92.

Green, J. L., J. Fan, and C. A. Angell. 1994. The protein-glass analogy: some insights from homopeptide comparisons. *J. Phys. Chem.* 98: 13780–13790.

Hage, W., A. Hallbrucker, E. Mayer, and G. P. Johari. 1994. Crystallization kinetics of water below 150 K. *J. Chem. Phys.* 100:2743–2747.

Hallbrucker, A., E. Mayer, and G. P. Johari. 1989. The heat capacity and glass transition of hyperquenched glassy water. *Phil. Mag.* 60B: 179–187.

Hallbrucker, A., E. Mayer, L. P. O'Mard, J. C. Dore, and P. Chieux. 1991. Structural characterisation of hyperquenched glassy water and vapour-deposited amorphous ice. *Phys. Lett. A.* 159:406–410.

Handa, Y. P., D. D. Klug, and E. Whalley. 1986. Difference in energy between cubic and hexagonal ice. *J. Chem. Phys.* 84:7009–7010.

Handa, Y. P., M. Zakrzewski, and C. Fairbridge. 1992. Effect of restricted geometries on the structure and thermodynamic properties of ice. *J. Phys. Chem.* 96:8594–8599.

Hofer, K., G. Astl., E. Mayer, and G. P. Johari. 1991. Vitrified dilute aqueous solutions. IV. Effects of electrolytes and polyhydric alcohols on the glass transition features of hyperquenched aqueous solutions. *J. Phys. Chem.* 95:10777–10781.

Hofer, K., A. Hallbrucker, E. Mayer, and G. P. Johari. 1989. Vitrified dilute aqueous solutions. III. Plasticization of water's H-bonded network and the glass transition temperature's minimum. *J. Phys. Chem.* 93: 4674–4677.

Hofer, K., E. Mayer, and I. M. Hodge. 1992. Physical ageing and modelling of the glass-liquid transition of water and aqueous solutions imbibed in poly-(2-hydroxyethyl-methacrylate) and in the bulk state. *J. Non-Crystall. Solids.* 139:78–85.

Hofer, K., E. Mayer, and G. P. Johari. 1990. Glass-liquid transition of water and ethylene glycol solution in poly(2-hydroxyethyl methacrylate) hydrogel. *J. Phys. Chem.* 94:2689–2696.

Jeffrey, G. A., and W. Saenger. 1994. Hydrogen Bonding in Biological Structures. Springer Verlag, Berlin. Chaps. 23 and 25.

Johari, G. P. 1987. Secondary relaxations and the properties of glasses and liquids. *In* Lecture Notes in Physics Series, Vol. 227. Springer Verlag, Heidelberg. 90–112.

Johari, G. P. 1993. A defect theory for the glass transition and residual entropy of hyperquenched water. *J. Chem. Phys.* 98:7324–7329.

Johari, G. P., and M. Goldstein. 1970. Viscous liquids and the glass transition. II. Secondary relaxations in glasses of rigid molecules. *J. Chem. Phys.* 53:2372–2388.

Johari, G. P., A. Hallbrucker, and E. Mayer. 1987. The glass transition of hyperquenched water. *Nature.* 330:552–553.

Johari, G. P., A. Hallbrucker, and E. Mayer. 1990. Isotope effect on the glass transition and crystallization of hyperquenched glassy water. *J. Chem. Phys.* 92:6742–6746.

Kauzmann, W. 1948. The nature of the glassy state and the behaviour of liquids at low temperatures. *Chem. Rev.* 43:219–256.

Kimmich, R. 1993. Self-diffusion and NMR relaxation in hydration shells of proteins. *In* Water-Biomolecule Interactions, Conference Proceedings, Vol. 43. M. U. Palma, M. B. Palma-Vittorelli, and F. Parak, editors. SIF, Bologna. 157–164.

Kimmich, R., T. Gneiting, K. Kotitschke, and G. Schnur. 1990. Fluctuations, exchange processes, and water diffusion in aqueous protein systems. *Biophys. J.* 58:1183–1197.

Kotitschke, K., R. Kimmich, E. Rommel, and F. Parak. 1990. NMR study of diffusion in protein hydration shells: observation of percolation transitions. *Prog. Colloid Polymer Sci.* 83:211–215.

Kuntz, I. D., and W. Kauzmann. 1974. Hydration of proteins and polypeptides. *Adv. Protein Chem.* 28:239–345.

Lounnas, V., B. M. Pettitt, and G. N. Phillips, Jr. 1994. A global model of the protein-solvent interface. *Biophys. J.* 66:601–614.

Mark, J. E., A. Eisenberg, W. W. Graessley, L. Mandelkern, E. T. Samulski, J. L. Koenig, and G. D. Wignall. 1993. Physical Properties of Polymers (ACS Professional Reference Book). American Chemical Society, Washington, DC. 89.

Mayer, E. 1994a. Hyperquenched glassy bulk water: a comparison with other amorphous forms of water; and with vitreous but freezable water in a hydrogel and on hydrated methemoglobin. *In* Water-Biomolecule Interactions, Conference Proceedings, Vol. 43. M. U. Palma, M. B. Palma-Vittorelli, and F. Parak, editors. SIF, Bologna. 355–372.

Mayer, E. 1994b. FTIR spectroscopic study of the dynamics of conformational substates in hydrated carbonyl-myoglobin films via temperature dependence of the CO stretching band parameters. *Biophys. J.* 67: 862–873.

Mayer, E. 1994c. "Freezing-in" of carbonylhemoglobin's CO conformer population by hyperquenching of its aqeous solution into the glassy state: an FTIR spectroscopic study of the limits of cryofixation. *J. Am. Chem. Soc.* 116:10571–10577.

Mayer, E., and G. Astl. 1992. Limits of cryofixation as seen by Fourier transform infrared spectra of metmyoglobin azide and carbonyl hemoglobin in vitrified and freeze-concentrated aqueous solution. *Ultramicroscopy.* 45:185–197.

Morozov, V. N., and S. G. Gevorkian. 1985. Low-temperature glass transition in proteins. *Biopolymers.* 24:1785–1799.

Moynihan, C. T., A. J. Easteal, M. A. deBolt, and J. Tucker. 1976. Dependence of the fictive temperature of glass on cooling rate. *J. Am. Ceram. Soc.* 59:12–16.

Mrevlishvili, G. M. 1979. Low-temperature calorimetry of biological macromolecules. *Sov. Phys. Usp.* 22:433–455.

Nienhaus, G. U., J. Heinzl, E. Huenges, and F. Parak. 1989. Protein crystal dynamics studied by time-resolved analysis of x-ray diffuse scattering. *Nature.* 338:665–666.

Olsen, K. W. 1994. Thermal denaturation procedures for hemoglobin. *Methods Enzymol.* 231:514–524.

Parak, F. 1986. Correlation of protein dynamics with water mobility: Mössbauer spectroscopy and microwave absorption methods. *Methods Enzymol.* 127:196–206.

Pethig, R. 1992. Protein-water interactions determined by dielectric methods. *Annu. Rev. Phys. Chem.* 43:177–205.

Pissis, P., A. Anagnostopoulou-Konsta, L. Apekis, D. Daoukaki-Diamanti, and C. Christodoulides. 1992. Dielectric studies on glass transitions in biological systems. *IEEE Trans. Electrical Insulation.* 27:820–825.

Plattner, H., and L. Bachmann. 1982. Cryofixation: a tool in biological ultrastructural research. *Int. Rev. Cytol.* 79:237–304.

Poole, P. L., and J. L. Finney. 1986. Solid-phase protein hydration studies. *Methods Enzymol.* 127:284–293.

Poole, P. L., A. R. Walton, and J. Z. Zhang. 1987. Crystallographic estimation of the non-freezing fraction of water in lysozyme. *Int. J. Biol. Macromol.* 9:245–246.

Rothgeb, T. M., and F. R. N. Gurd. 1978. Physical methods for the study of myoglobin. *Methods Enzymol.* 52:473–486.

Rupley, J. A., and G. Careri. 1991. Protein hydration and function. *Adv. Protein Chem.* 41:37–172.

Rupley, J. A., E. Gratton, and G. Careri. 1983. Water and globular proteins. *Trends Biol. Sci.* 8:18–22.

Sartor, G. 1991. Untersuchungen von vitrifizierbarem Wasser an Methämoglobin und Lysozym mit Differentieller Scanning Kalorimetrie und Röntgenbeugung. Diplomarbeit. Universität Innsbruck, Innsbruck, Austria.

Sartor, G. 1994. Kalorimetrische Untersuchungen der Dynamik von Wasser und Protein in hydratisierten Methämoglobin-, Metmyoglobin- und Lysozym-Pulvern. Ph.D. thesis. Universität Innsbruck, Innsbruck, Austria.

Sartor G., A. Hallbrucker, K. Hofer, and E. Mayer. 1992. Calorimetric glass-liquid transition and crystallization behavior of a vitreous, but freezable, water fraction in hydrated methemoglobin. *J. Phys. Chem.* 96:5133–5138.

Sartor, G., A. Hallbrucker, K. Hofer, and E. Mayer. 1993. Glass-liquid transition and crystallization of a vitreous, but freezable, water fraction in hydrated methemoglobin. *In* Water-Biomolecule Interactions, Conference Proceedings, Vol. 43. M. U. Palma, M. B. Palma-Vittorelli, and F. Parak, editors. SIF, Bologna. 143–146.

Sartor, G., and E. Mayer. 1994. Calorimetric study of crystal growth of ice in hydrated methemoglobin and of redistribution of the water clusters formed on melting the ice. *Biophys. J.* 67:1724–1732.

Sartor, G., E. Mayer, and G. P. Johari. 1994. Calorimetric studies of the kinetic unfreezing of molecular motions in hydrated lysozyme, hemoglobin, and myoglobin. *Biophys. J.* 66:249–258.

Smith, J., K. Kuczera, and M. Karplus. 1990. Dynamics of myoglobin: comparison of simulation results with neutron scattering spectra. *Proc. Natl. Acad. Sci. USA.* 87:1601–1605.

Smyth, G., F. X. Quinn, and V. J. McBrierty. 1988. Water in hydrogels. II. A study of water in poly(hydroxyethyl methacrylate). *Macromolecules.* 21:3198–3204.

Srajer, V., L. Reinisch, and P. M. Champion. 1991. Investigation of laser-induced long-lived states of photolyzed MbCO. *Biochemistry.* 30: 4886–4893.

Stephens, R. B. 1976. Relaxation effects in glassy selenium. *J. Non-Crystall. Solids.* 20:75–81.

Teeter, M. M. 1991. Order and disorder in water structure of crystalline proteins. *Dev. Biol. Standard.* 74:63–72.

Uhlman, D. R. 1972. A kinetic treatment of glass formation. *J. Non-Crystall. Solids* 7:337–348.

Uhlmann, D. R., and H. Yinnon. 1983. The Formation of glasses. *In* Glass: Science and Technology, Vol. 1. D. R. Uhlmann and N. J. Kreidl, editors. Academic Press, New York. 21.

Waterman, M. R. 1978. Spectral characterization of human hemoglobin and its derivatives. *Methods Enzymol.* 52:456–463.

Wong, J., and C. A. Angell. 1976. Glass-Structure by Spectroscopy. Dekker, New York. Chap. 1.

Wunderlich, B. 1960. Study of the change in specific heat of monomeric and polymeric glasses during the glass transition. *J. Phys. Chem.* 64: 1052–1056.

Yang, P.-H., and J. A. Rupley. 1979. Protein-water interactions: heat capacity of the lysozyme-water system. *Biochemistry.* 18:2654–2661.